Indium Phosphide Photonic Integrated Circuits: Technology and Applications

Jonathan Klamkin
Electrical and Computer Engineering Department
University of California Santa Barbara
Santa Barbara, USA
klamkin@ece.ucsb.edu

Hongwei Zhao
Electrical and Computer Engineering Department
University of California Santa Barbara
Santa Barbara, USA
hwzhao@ece.ucsb.edu

Bowen Song
Electrical and Computer Engineering Department
University of California Santa Barbara
Santa Barbara, USA
bowen@ece.ucsb.edu

Yuan Liu
Electrical and Computer Engineering Department
University of California Santa Barbara
Santa Barbara, USA
yuan.liu@umail.ucsb.edu

Brandon Isaac
Materials Department
University of California Santa Barbara
Santa Barbara, USA
brandonjisaac@umail.ucsb.edu

Sergio Pinna
Electrical and Computer Engineering Department
University of California Santa Barbara
Santa Barbara, USA
pinna@ece.ucsb.edu

Fengqiao Sang
Electrical and Computer Engineering Department
University of California Santa Barbara
Santa Barbara, USA
fsang@umail.ucsb.edu

Larry Coldren
Electrical and Computer Engineering and Department
University of California Santa Barbara
Santa Barbara, USA
coldren@ece.ucsb.edu

***Abstract*—A summary of photonic integrated circuit (PIC) platforms is provided with emphasis on indium phosphide (InP). Examples of InP PICs were fabricated and characterized for free space laser communications, Lidar, and microwave photonics. A novel high-performance hybrid integration technique for merging InP devices with silicon photonics is also discussed.**

Keywords—photonic integrated circuit, indium phosphide, silicon photonics, silicon nitride, hybrid integration.

I. INTRODUCTION

Photonic integrated circuit (PIC) technology continues to mature and expand in terms of functionality and performance [1]. Although silicon photonics (SiPh) has gained traction and promises low-cost and high-volume production, indium phosphide (InP) continues to be the most popular and advanced PIC platform [2], [3]. Also, currently all SiPh PICs utilize either InP or gallium arsenide (GaAs) lasers for optical sources and rely on external coupling or heterogeneous/hybrid integration.

Silicon nitride (SiN) has also received significant attention as a low-loss passive waveguide PIC platform [4], [5]. Lastly, lithium niobate (LN) continues to be used widely for high-speed modulators for telecommunications.

Figure 1 summarizes the primary PIC platforms illustrating common waveguide geometries used for each. The structure illustrated in Fig. 1(a) is referred to as a ridge or rib waveguide. A common waveguide core is indium gallium arsenide phosphide (InGaAsP) while the cladding material is InP. Depending on layer composition, thickness, and feature size, the waveguide core optical confinement is considered to be moderate for InP. This directly determines the size/compactness of passive components and is also an important consideration for the efficiency of active devices. InP allows for the integration of all active components including lasers, semiconductor optical amplifiers (SOAs), photodetectors, and modulators. Depending on the complexity of the active-passive integration approach, low passive waveguide loss can also be demonstrated.

SiPh is based on silicon on insulator (SOI) technology and is illustrated in Fig. 1(b). Modulators based on pn junctions and germanium photodetectors have become mainstay active components for SiPh. The most common silicon device layer thickness is 220 nm and the buried oxide (BOX) layer is typically 2-3 μm. This platform is characteristic of very high index contrast (the refractive indices of the silicon core and oxide cladding are approximately 3.5 and 1.5, respectively at a wavelength of 1.55 μm) and therefore passive component sizes are extremely small. Unfortunately, modulation mechanisms in silicon are weak, therefore modulators are large in size despite the high index contrast. SiPh also lacks an inherent laser technology and therefore techniques have been developed to integrate compound semiconductor materials such as InP to provide gain.

SiN can be considered as an alternative to traditional glass waveguide technology that is based on doped silica. This is a passive PIC platform that could rely on hybrid or heterogeneous approaches to closely integrate active components. SiN is used as the core guiding material and silicon dioxide as the cladding material. Thicker waveguide cores (200-400 nm) can realize relatively strong optical confinement and in turn sharp waveguide bends and compact components [6]. Thinner SiN cores (40-100 nm) can realize more loosing confined waveguide modes and extremely low passive loss [7].

The next section will focus on the high-performance InP PIC platform, detailing the variety of components available as well as common active-passive integration techniques therein.

978-1-5386-6502-2/18/$31.00 ©2018 IEEE

II. Indium Phoshpide PICs

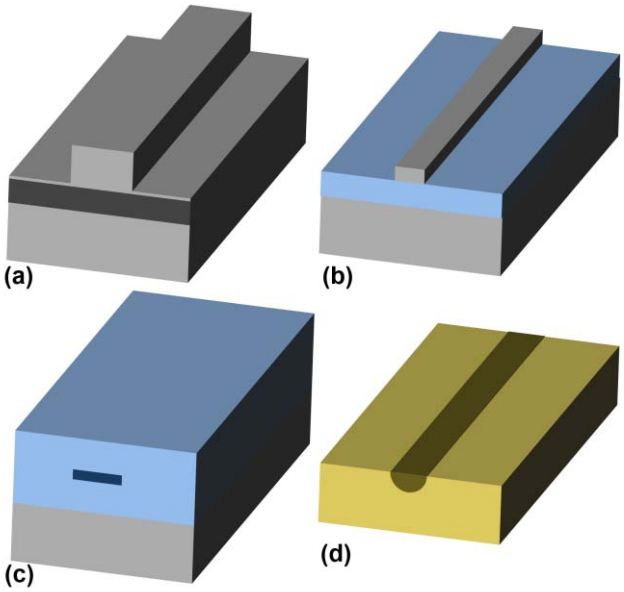

Fig. 1. Summary of PIC platforms: (a) InP, (b) SiPh, (c) SiN, (d) LN.

InP can realize lasers emitting in the common telecommunications bands between 1.26-1.625 µm. Additionally, high-performance modulators and photodetectors can be realized with this material system, therefore it represents an ideal PIC platform to reduce photonic system cost, size, weight and power (CSWaP).

Many InP lasers are based on strained multi-quantum well (MQW) active regions. The lasers types that are available include distributed feedback (DFB) and several distributed Bragg reflector (DBR) variants [8]. One of the more mature widely tunable lasers is the sampled grating DBR (SGDBR) laser [9]. To effectively realize such a multi-section DBR

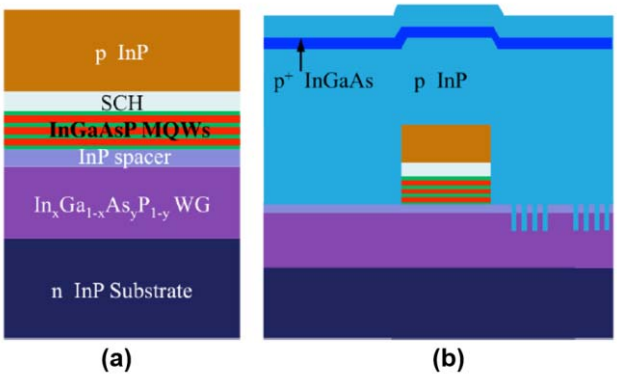

Fig. 2. Illustration of InP OQW PIC platform. (a) Cross section schematic of base epitaxial wafer. (b) Side view schematic after active passive-passive definition, grating formation, and p-cladding regrowth.

laser, an active-passive integration technique is required to selectively form regions for gain and regions that are optically transparent to the laser emission wavelength. The offset quantum well (OQW) platform provides a robust method for achieving this. Figure 2(a) shows a cross section schematic of the base epitaxial structure whereby the quantum wells are deposited on top of a waveguide core in such a way that the quantum wells are offset spatially from the peak of the waveguide optical mode. For active-passive integration, the

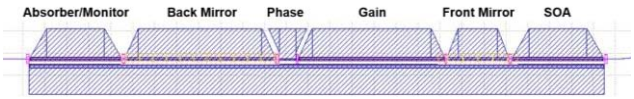

Fig. 3. Layout of multi-section SGDBR laser.

quantum wells are removed selectively. The DBR gratings are etched into the top of the waveguide layer and then the p-InP cladding and p-indium gallium arsenide (InGaAs) contact layers are deposited in a regrowth step. A side view schematic following this step is shown in Fig. 2(b). The remaining fabrication steps include ridge formation, passivation, and metal contact formation.

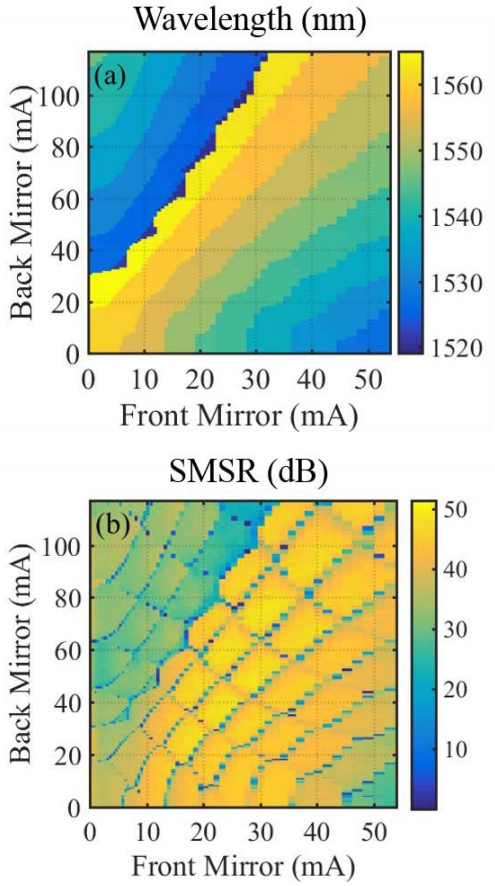

Fig. 4. SGDBR laser wavelength (a) and SMSR (b) as a function of applied back and front mirror currents.

InP PICs were initially developed primarily for telecommunications and have matured substantially due to the steady growth of this industry [10]. Other application areas have leveraged this technology, making use of the abundance of commercial-off-the-shelf (COTS) components. Examples are microwave photonics, and free space laser communications and sensing [11], [12]. These applications

would benefit greatly from PIC technology to reduce system CSWaP. This would allow for more frequent deployments and integration on smaller platforms.

Specifically, for space optical communications, InP PICs have been developed recently with the OQW platform and SGDBR laser sources [13], [14]. A layout schematic of an SGDBR laser is illustrated in Fig. 3. The laser consists

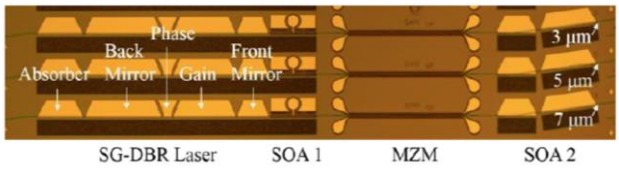

Fig. 5. Microscope images of InP PIC transmitters.

minimally of a gain section, a front SGDBR mirror, a back SGDBR mirror, and a gain section. Also common are to include an output SOA and a back absorber that can be used as a monitor photodetector. These lasers output well above 15 mW of optical power, and the power level is increased with the use of the output SOA. The lasers also tune over more than

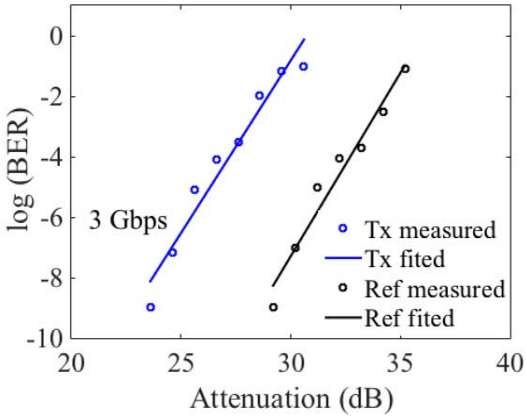

Fig. 6. BER measurements comparing PIC transmitter to reference.

45 nm and demonstrate high side-mode suppression ratio (SMSR) across this tuning range, as illustrated in Fig. 4. For high-speed transmitters, Mach-Zehnder modulators (MZMs) were integrated. The modulation mechanism is based on the Franz-Keldysh effect and utilizes the pn junction formed with the bulk InGaAsP waveguide core. As shown in Fig. 5, additional high-power two-section SOAs were incorporated at the output following the MZMs. The second SOAs in some cases have flared outputs with widths that are 5 µm or 7 µm to increase the saturation power level.

The transmitters were characterized in a free space link. A 3 Gbps non-return-to-zero (NRZ) pseudo random binary sequence (PRBS) was generated and applied to the MZM. The optical signal from the transmitter was collected by a lensed single mode fiber (SMF) and coupled to an optical collimator with a beam divergence angle of 0.016°, and then transmitted through air. At the receiver, an identical collimator collected the light. The distance between the collimators was 1.35 m. An in-fiber variable optical attenuator (VOA) was used to emulate free space link attenuation. The bit error rate (BER) was measured for the PIC transmitter and compared to a reference consisting of an external cavity laser and high-speed LN modulator. The results are shown in Fig. 6. illustrating error free operation (BER < 1×10^{-9}) for up to approximately 24 dB attenuation (180 m distance). With forward error correction (BER < 2×10^{-3}), the equivalent link length can be up to 300 m (28 dB attenuation). In both cases, with a high-power booster amplifier the link distance can be increased significantly.

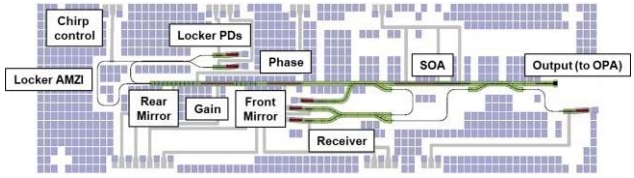

Fig. 7. InP PIC transceiver for beamsteering Lidar.

In addition to free space laser communications, InP PICs can enable a number of other emerging applications including Lidar, microwave photonics, and remote sensing. For some applications, the integration of InP with SiPh is desirable and can also facilitate packaging and electronic-photonic integration. Section III will discuss techniques to integrate InP lasers and PICs, such as those described, with SiPh.

An example of an InP PIC transceiver for a beamsteering Lidar system is shown in Fig. 7. This PIC comprises of a widely tunable SGDBR laser, a frequency discriminator for

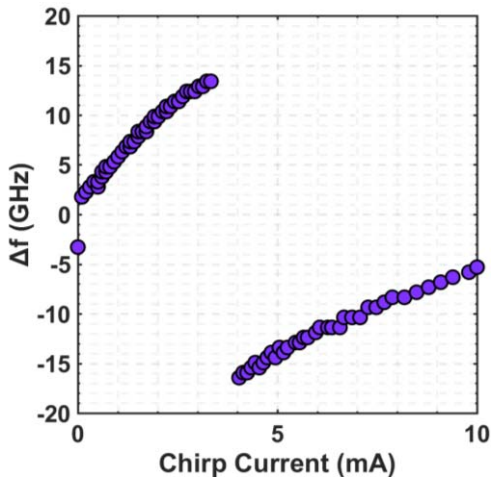

Fig. 8. Demonstration of locking functionality and application of chirp.

wavelength locking/stabilization, and a balanced receiver for coherent detection [15], [16]. This transceiver was designed to drive an optical phased array (OPA) for 3D mapping and other Lidar applications. Light from this PIC would couple to a SiPh circuit that includes a star coupler and a large array of phase shifters and (wavelength-dependent) grating emitters. 2D beam steering is achieved through the combination of the 1D phased array and wavelength tuning. The SGDBR laser is ideal for this application because of its wide tuning range. A frequency discriminator based on an asymmetric Mach-

Zehnder interferometer (AMZI) is used in conjunction with photodiodes (PDs) and an electronic circuit based amplifier/filter that drives the phase section of the laser to stabilize the wavelength between tuning steps. A chirp signal (frequency modulation) can be applied with a phase shifter implemented in one arm of the AMZI to enable a frequency-modulated continuous wave (FMCW) Lidar system. Figure 8 shows measurement results to demonstrate the locking functionality and application of chirp. First the laser is tuned to a specific wavelength using a lookup table (similar to the tuning map illustrated in Fig. 4). Then the AMZI-based locker would stabilize the wavelength, and following this the frequency modulation is generated by applied a small signal to the chirp control. The PIC also contains a balanced receiver that mixes a portion of the on-chip SGDBR laser power (serving as a local oscillator) with the return signal that is coupled through the same OPA.

III. Hybrid Inegration For SiPh

For SiPh, several approaches to laser integration have been pursued including monolithic integration by heteroepitaxy, co-packaging, heterogeneous wafer bonding, and hybrid flip-chip

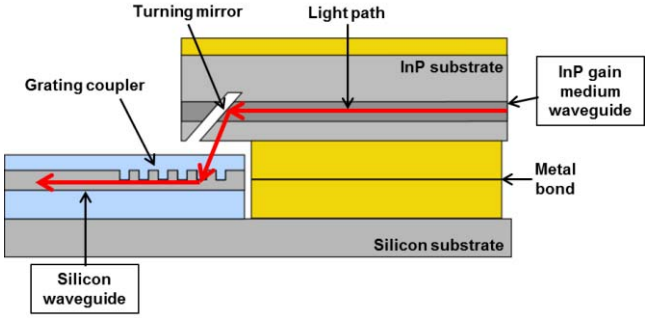

Fig. 9. 3D photonic integration platform.

integration. In addition to employing these techniques for integration of the laser source or sources, they can also enable the integration of full InP PICs on SiPh or SiN interposers. This is desirable for applications requiring the close integration of high-performance PICs with low-loss waveguide passive components, and to facilitate electronic-photonic integration and packaging.

Laser integration by heteroepitaxy of InP, GaAs and related compounds on silicon is promising for large-scale PICs. Although continuous wave (CW) lasing has been demonstrated, there are a number of challenges to overcome to improve reliability [17], [18].

Co-packaging involves the use of bulk optics to couple light from a semiconductor laser chip to a SiPh circuit. This technique has been utilized in industry [19]. It is advantageous because it allows for the use of qualified laser chips, but requires somewhat expensive assembly processes. This is also characteristic of limited scalability.

Heterogeneous approaches are based on wafer bonding and subsequent co-fabrication [20]. Typically, InP chiplets are bonded, the InP substrate is removed, and then mesas pin diode structures are fabricated to facilitate electrically pumped lasing.

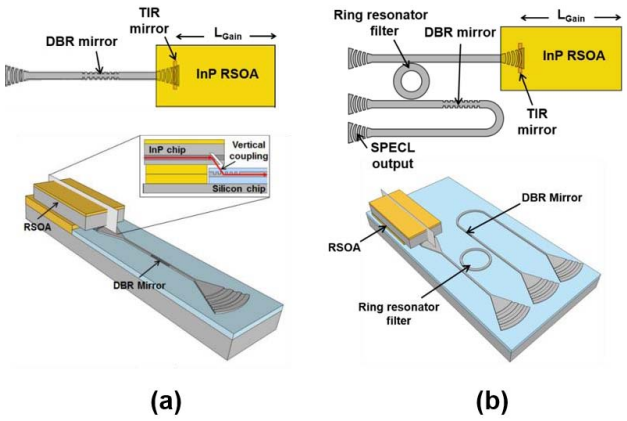

Fig. 10. SPECL with a DBR mirror only (a) and with both a DBR mirror and intra-cavity ring resonator filter (b).

The co-fabrication likely requires utilization of a silicon facility for the underlying SOI waveguide formation, and a separate facility for the InP fabrication. This platform does not require precision alignment of the InP chips for bonding. In addition to lasers and SOAs, the InP chiplets can be used for other active components including modulators and photodetectors, both of which arguably outperform their silicon counterpart. Although this technique is promising, co-fabrication is expensive and the performance is limited. Thick SOI waveguides are required to ensure coupling from the InP, as is a thick BOX layer for preventing substrate leakage. The BOX layer thermally isolates the InP active region leading to a high internal temperature under operation and low laser efficiency. Lastly, the mismatch in coefficient of thermal expansion potentially poses reliability issues [21].

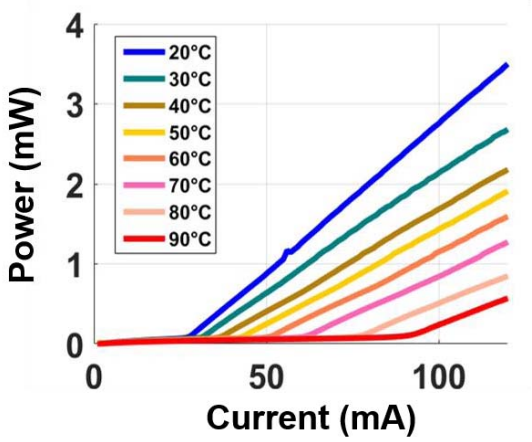

Fig. 11. Light-current characteristics for 3D hybrid laser at various operating temperatures.

Hybrid integration involves the close integration of separate laser chips and SiPh circuits [22]. In some cases, other intermediate chip-scale optics can be integrated on chip including isolators [23]. As for co-packaging, hybrid integration also uses fully fabricated laser chips, albeit perhaps with some customization, and avoids co-fabrication of dissimilar materials. Flip-chip integration can overcome

thermal issues since the InP chip can be directed bonded (or nearly directly bonded) to the silicon substrate, ensuring effective extraction of heat from the active region and dissipation into the highly thermally conductive silicon. A primary concern for planar butt-coupling of InP to SiPh is the alignment precision required because planar laser diodes are characteristic of large angular beam divergence, especially in the vertical direction [24]. The 3D hybrid integration approach overcomes some of these issues [25]. As illustrated in Fig. 7, InP devices (lasers or PICs) with fabricated with total internal reflection (TIR) turning mirrors to incorporate surface emission into the planar device. This is then flip-chip bonded to the

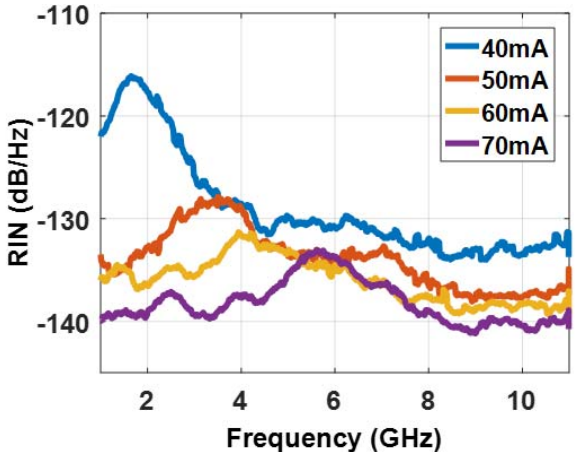

Fig. 12. RIN spectra for 3D hybrid laser at various operating current.

silicon and light is coupled into the SOI waveguide through a surface grating coupler, which is commonly employed for fiber coupling.

With this technology, either a standalone laser can be integrated, or a gain element can be integrated. For the latter, a reflective SOA (RSOA) can be integrated to provide gain, and feeback/filtering elements can be formed in the SiPh. Figure 8 depicts two types of such silicon photonic external cavity lasers (SPECLs), one that includes a single DBR mirror in the silicon, and the other that includes both a DBR mirror and an intra-cavity ring resonator filter [26]. Both lasers demonstrate single-mode lasing and some tunability because the DBRs and ring resonators in silicon include micro-heaters for thermal tuning.

Since the RSOAs were flip-chip bonded p-side down directly to the silicon substrate, heat generated in the InP active region is extracted effectively and dissipated in the silicon. In addition to perform thermal simulations to demonstrate this, an experiment was conducted to compare an InP device bonded to the top oxide cladding (and thermally isolated from the silicon substrate), to one bonded directly to the silicon. The latter demonstrated a thermal impedance that was a factor of three lower. Additionally, as illustrated in Fig. 9, these lasers operated at high temperature with an efficiency that is not severely degraded. Lastly, to provide an initial investigation into laser performance for communications applications, the relative intensity noise (RIN) was measured for a SPECL and the results are shown in Fig. 10. The RIN was less than -135 dB/Hz for a drive current of 70 mA.

Hybrid integration generally can also be leveraged to integrate not only lasers and SOAs, but also complex InP PICs such as those described in the previous section, and other high-performance active devices such as PDs. Figure 13 illustrates a concept for an optical beam forming network (OBFN) chip for high-frequency wireless communications and phased arrays

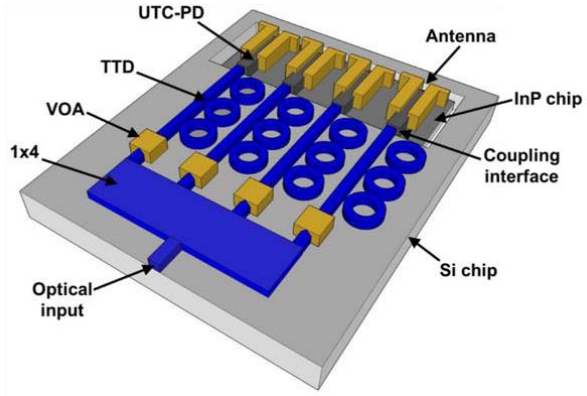

Fig. 13. OBFN chip concept.

[27]. For wireless, photonics is attractive for its broad bandwidth and immunity to electromagnetic interference [28]. The OBFN chip concept comprises all of the components required for signal generation, distribution, and radiation. The distribution network is based on an array of true time delay (TTD) elements for beamsteering to eliminate the beam squint issue associated with RF phase shifters. This TTD technology is now well developed and has been implemented on low-loss waveguide platforms on silicon [4], [29], [30]. Critical to such a system are the high-speed PDs required for mixing optical signals to generate the high-frequency signal to be radiated from the phased array antenna. InP-based uni-traveling-carrier photodiodes (UTC-PDs) are most ideal for this application for their ability to generate reasonable power levels while maintaining millimeter wave (mmW) class bandwidth and beyond [31], [32], [33]. To enable integration of such PDs with low-loss waveguides on silicon, as desired for the integrated OBFN concept, UTC-PDs were developed for integration with spot-size converters (SSCs) to enable hybrid integration and high efficiency coupling. Preliminary results have demonstrated 3-dB bandwidth as high as 67 GHz and 50 Gb/s on-off keying (OOK) operation. Future work will be focused on increasing the bandwidth and data rate further, as well as the hybrid integration of these PDs on silicon.

IV. Conclusions

InP PIC technology has been reviewed and some examples were described in detail, including a PIC transmitter for free space optical communications and a PIC transceiver for Lidar. A novel 3D hybrid integration approach was also discussed in the context of InP laser and PIC integration on SiPh. And lastly, a concept for integrating high-performance InP PDs for mmW communications and phase arrays was discussed.

Acknowledgment

The authors acknowledge the NASA Space Technology Mission Directorate (STMD) for support.

REFERENCES

[1] Y. A. Vlasov, "Silicon CMOS-integrated nano-photonics for computer and data communications beyond 100G," IEEE Communications Magazine, vol. 50, no. 2, pp. s67-s72, 2012.

[2] V. Lal, et al., "Extended C-Band Tunable Multi-Channel InP-Based Coherent Transmitter PICs, vol. 35, no. 7, pp. 1320-1327, 2017.

[3] S. Arafin, L. A. Coldren, "Advanced InP Photonic Integrated Circuits for Communication and Sensing," IEEE Journal of Selected Topics in Quantum Electronics, vol. 24, no. 1, 2018.

[4] Y. Liu, A. Wichman, B. Isaac, J. Kalkavage, E. Adles, J. Klamkin, "Ring Resonator Delay Elements for Integrated Optical Beamdorming Networks: Group Delay Ripple Analysis," Integrated Photonics Research, Silicon and Nanophotonics Conference, paper IW1B.3, 2016.

[5] C. G. H. Roeloffzen, L. Zhuang, C. Taddei, A. Leinse, R. G. Heideman, P. W. L. van Dijk, R. M. Oldenbeuving, D. A. I. Marpaung, M. Burla, K. –J. Boller, "Silicon nitride microwave photonic circuits," Optics Express, vol. 21, no. 19, pp. 22937-22961, 2013.

[6] S. Dwivedi, B. Song, Y. Liu, R. Mereira, L. Johansson, J. Klamkin, "Demonstration of compact silicon nitride grating coupler arrays for fan-out of multicore fibers," Conference on Lasers and Electro-Optics, paper ATh3B.4, 2017.

[7] J. F. Bauters, M. J. R. Heck, D. D. John, J. S. Barton, C. M. Bruinink, A. Leinse, R. G. Heideman, D. J. Blumenthal, J. E. Bowers, "Planar wavegides with less than 0.1 dB/m propagation loss fabricated with wafer bonding," Optics Express, vol. 19, no. 24, pp. 24090-24101, 2011.

[8] L. A. Coldren, S. W. Corzine, M. L. Masanovic, Diode Lasers and Photonic Integrated Circuits. Hoboken, NJ: John Wiley & Sons, 2012.

[9] L. A. Coldren, G. A. Fish, Y. Akulova, J. S. Barton, L. Johansson, C. W. Coldren, "Tunable Semiconductor Lasers: A Tutorial," Journal of Lightwave Technology, vol. 22, no. 1, pp. 193-202, 2004.

[10] T. L. Koch, U. Koren, "InP-based photonic integrated circuits," IEEE Procedings, vol. 138, no. 2, pp. 139-147, 1991.

[11] S. Iezekiel, M. Burla, J. Klamkin, D. Marpaung, J. Capmany, "RF Engineering Meets Optoelectronics: Progress in Integrated Microwave Photonics," IEEE Microwave Magazine, vol. 16, no. 8, 2015.

[12] V. W. S. Chan, "Free-Space Optical Communications," Journal of Lightwave Technology, vol. 24, no. 12, pp. 4750-4762, 2006.

[13] H. Zhao, S. Pinna, B. Song, L. Megalini, S. T. Suran Brunelli, L. Coldren, J. Klamkin, "Indium Phosphide Photonic Integrated Circuits for Free Space Optical Links," IEEE Journal of Selected Topics in Quantum Electronics, 2018.

[14] H. Zhao, S. Pinna, B. Song, L. Megalini, S. T. Suran Brunelli, L. Coldren, J. Klamkin, "High-Power Integrated Indium Phosphide Transmitter for Free Space Optical Communications," Conference on Lasers and Electro-Optics, paper JW2A.52, 2018.

[15] B. Isaac, B. Song, S. Pinna, S. Arafin, L. Coldren, J. Klamkin, "Indium Phosphide Photonic Integrated Circuit Transmitter with Integrated Linewidth Narrowing for Laser Communications and Sensing," International Semiconductor Laser Conference, 2018.

[16] Y. Zhang, Y. –C. Ling, Y. Zhang, K. Shang, S. J. Ben Yoo, "High-Density Wafer-Scale 3-D Silicon-Photonic Integrated Circuits," IEEE Journal of Selected Topics in Quantum Electronics, vol. 24, no. 6, 2018.

[17] L. Megalini, B. Bonef, B. C. Cabinian, H. Zhao, A. Taylor, J. S. Speck, J. E. Bowers, J. Klamkin, Appl. Phys. Lett. 111, 032105, 2017.

[18] S. Chen, W. Li, J. Wu, Q. Jiang, M. Tang, S. Shutts, S. N. Elliott, A. Sobiesierski, A. J. Seeds, I. Ross, P. M. Smowton, H. Liu, "Electrically pumped continuous-wave III-V quantum dot lasers on silicon," Nature Photonics, vol. 10, pp. 307-311, 2016.

[19] T. Pinguet, P. M. De Dobbelaere, D. Foltz, S. Gloeckner, S. Hovey, Y. Liang, M. Mack, G. Masini, A. Mekis, M. Peterson, T. Pinguet, S. Sahni, J. Schramm, M. Sharp, L. Verslegers, B. P. Welch, K. Yokoyama, S. Yu, "25 Gb/s silicon photonic transceivers," International Conference on Group IV Photonics, 2012.

[20] A. W. Fang, H. Park, O. Cohen, R. Jones, M. J. Paniccia, J. E. Bowers, "Electrically pumped hybrid AlGaInAs-silicon evanescent laser," Optics Express, vol. 14, no. 20, pp. 9203-9210, 2006.

[21] B. Song, L. Megalini, S. Dwivedi, S. Ristic, J. Klamkin, "High-Thermal Performance 3D Hybrid Silicon Lasers," IEEE Photonics Technology Letters, vol. 29, no. 14, pp. 1143-1146, 2017.

[22] A. Rickman, "The commercialization of silicon photonics," Nature Photonics, vol. 8, pp. 79-582, 2014.

[23] M. Mazzini, M. Traverso, M. Webster, C. Muzio, S. Anderson, P. Sun, D. Siadat, D. Conti, A. Cervasio, S. Pfnuer, J. Stayt, M. Nyland, C. Togami, K. Yanushefski, T. Daugherty, "25GBaud PAM-4 error free transmission over both single mode fiber and multimode fiber in a QSFP form factor based on silicon photonics," Optical Fiber Communications Conference, 2015.

[24] N. Kobayashi, K. Sato, M. Namiwaka, K. Yamamoto, S. Watanabe, T. Kita, H. Yamada, and H. Yamazaki, "Silicon Photonic Hybrid Ring-Filter External Cavity Wavelength Tunable Lasers," *J. Lightwave Technol.*, vol. 33, no. 6, pp. 1241–1246, Mar. 2015.

[25] B. Song, C. Stagarescu, S. Ristic, A. Behfar, J. Klamkin, "3D integrated hybrid silicon laser," Optics Express, vol. 24, no. 10, pp. 10435-10444, 2016.

[26] B. Song, Y. Liu, S. Ristic, J. Klamkin, "Tunable 3D hybrid integrated silicon photonic external cavity laser," Conference on Lasers and Electro-Optics, paper AM4A.3, 2017.

[27] J. A. Nanzer, A. Wichman, J. Klamkin, T. P. McKenna, T. R. Clark, "Millimeter-Wave Photonic for Communications and Phased Arrays," Fiber and Integrated Optics, vol. 34, no. 4, pp. 159-174, 2015.

[28] G. Choo, C. K. Madsen, S. Palermo, K. Entesari, "Automatic Monitor-Based Tuning of RF Silicon Photonic True-Time-Delay Beamforming Networks," IEEE/MTT-S International Microwave Symposium, 2018.

[29] Y. Liu, A. R. Wichman, B. Isaac, J. Kalkavage, T. R. Clark, J. Klamkin, "Ultra-Low-Loss Silicon Nitride Optical Beamforming Network for Wideband Wirelss Applications," IEEE IEEE Journal of Selected Topics in Quantum Electronics, vol. 24, no. 4, 2018.

[30] Y. Liu, A. R. Wichman, B. Isaac, J. Kalkavage, T. R. Clark, J. Klamkin, "Tuning Optimization of Ring Resonator Delays for Integrated Optical Beam Forming Networks," Journal of Lightwave Technology, vol. 35, no. 22, pp. 4954-4960, 2017.

[31] J. Klamkin, A. Ramaswamy, L. A. Johansson, H. –F. Chou, M. N. Sysak, J. W. Raring, N. Parthasarathy, S. P. DenBaars, J. E. Bowers, L. A. Coldren, "High Output Saturation and High-Linearity Uni-Traveling-Carrier Waveguide Photodiodes," IEEE Photonics Technology Letters, vol. 19, no. 3, 2007.

[32] Z. Li, H. Pan, H. Chen, A. Beling, J. C. Campbell, "High-Saturation-Current Modified Uni-Traveling-Carrier Photodiode With Cliff Layer," IEEE Journal of Quantum Electronics, vol. 46, no. 5, pp. 626-632, 2010.

[33] B. Isaac, Y. Liu, B. Song, X. Xie, A. Beling, J. Klamkin, "Hybrid Integration of UTC-PDs on Silicon Photonics," Conference on Lasers and Electro-Optics, paper SM4O.1, 2017.